PERGAMON International Journal of Engineering Science 40 (2002) 1511–1527

International Journal of Engineering Science

www.elsevier.com/locate/ijengsci

MHD flow over a moving plate in a rotating fluid with magnetic field, Hall currents and free stream velocity

H.S. Takhar [a,*], A.J. Chamkha [b], G. Nath [c]

[a] *Department of Engineering, Manchester Metropolitan University, Oxford Road, Manchester M1 5GD, UK*
[b] *Department of Mechanical Engineering, Kuwait University, P.O. Box. 5969, Safat, Kuwait*
[c] *Department of Mathematics, Indian Institute of Science, Bangalore 560012, India*

Received 22 May 2001; accepted 1 August 2001

(Communicated by E.S. ŞUHUBİ)

Abstract

The non-similar boundary layer flow of a viscous incompressible electrically conducting fluid over a moving surface in a rotating fluid, in the presence of a magnetic field, Hall currents and the free stream velocity has been studied. The parabolic partial differential equations governing the flow are solved numerically using an implicit finite-difference scheme. The Coriolis force induces overshoot in the velocity profile of the primary flow and the magnetic field reduces/removes the velocity overshoot. The local skin friction coefficient for the primary flow increases with the magnetic field, but the skin friction coefficient for the secondary flow reduces it. Also the local skin friction coefficients for the primary and secondary flows are reduced due to the Hall currents. The effects of the magnetic field, Hall currents and the wall velocity, on the skin friction coefficients for the primary and secondary flows increase with the Coriolis force. The wall velocity strongly affects the flow field. When the wall velocity is equal to the free stream velocity, the skin friction coefficients for the primary and secondary flows vanish, but this does not imply separation. © 2002 Published by Elsevier Science Ltd.

1. Introduction

The rotating flow of an electrically conducting fluid in the presence of a magnetic field is encountered in cosmical and geophysical fluid dynamics. It can provide an explanation for the observed maintenance and secular variation of the geomagnetic field [1]. It is also important in the solar physics involved in the sunspot development, the solar cycle and the structure of rotating

* Corresponding author. Tel.: +44-161-247-3668; fax: +44-161-247-1633.
E-mail address: h.s.takhar@mmu.ac.uk (H.S. Takhar).

0020-7225/02/$ - see front matter © 2002 Published by Elsevier Science Ltd.
PII: S0020-7225(02)00016-2

magnetic stars [2]. The effect of the Coriolis force due to the earth's rotation is found to be significant as compared to the inertial and viscous forces in the equations of motion. The Coriolis and the electromagnetic forces are of comparable magnitude. The Coriolis force exerts a strong influence on the hydromagnetic flow in the earth's liquid core which plays an important role in the mean geomagnetic field [1]. The boundary layer flow on a stationary surface or in a channel in a rotating fluid with or without the presence of a magnetic field has been considered by a number of investigators [3–11].

Wang [12] has studied the steady flow on a stretching sheet in a rotating fluid. Takhar and Nath [13] have examined the effect of the magnetic field on a stretching sheet in a rotating fluid. The effect of the Hall currents on the MHD flow in a non-rotating system has also been investigated by several authors [14–19].

This paper aims to study the combined effects of the magnetic field, Hall currents and free stream velocity on the non-similar flow over a moving surface, in a rotating fluid. The parabolic coupled nonlinear partial differential equations governing the flow have been solved numerically using an implicit finite-difference scheme similar to that of Blottner [20]. The results have been compared with those of Kurosaka [6], Howarth [21], Tsou et al. [22], Chiam [23] and Lin and Huang [24].

2. Formulation

The physical model and the coordinate are given in Fig. 1, where x, y and z are the Cartesian coordinates and u, v and w are the velocity components along the x, y and z directions, respectively. Let us consider an insulated surface which coincides with the plane $z = 0$. This plane moves with a constant velocity U_1 in the x direction in a viscous, incompressible, electrically conducting fluid which is rotating with a constant angular Ω_0 about the z-axis. There exists a uniform free stream velocity U_2 parallel to the x-axis. The magnetic field B_0 is applied in the z-direction. All the physical properties of the fluid are assumed to be constant. The effects of Coriolis force and (or)

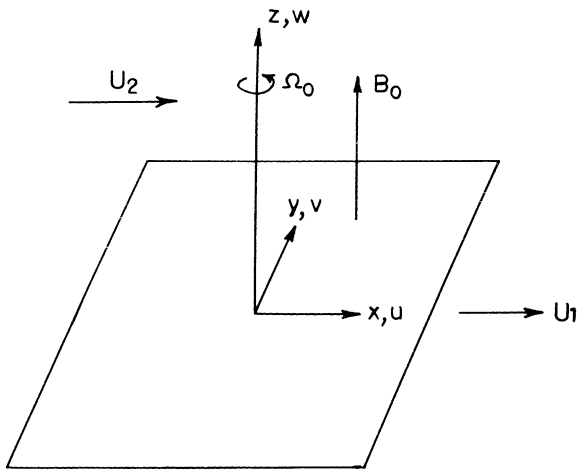

Fig. 1. Physical model and the coordinate system.

the Hall currents give rise to a force in y-direction, which induces a cross flow in that direction. Hence the flow becomes three-dimensional. The governing equations in a rotating frame of reference with Maxwell's electromagnetic equations are given by [5,6,25].

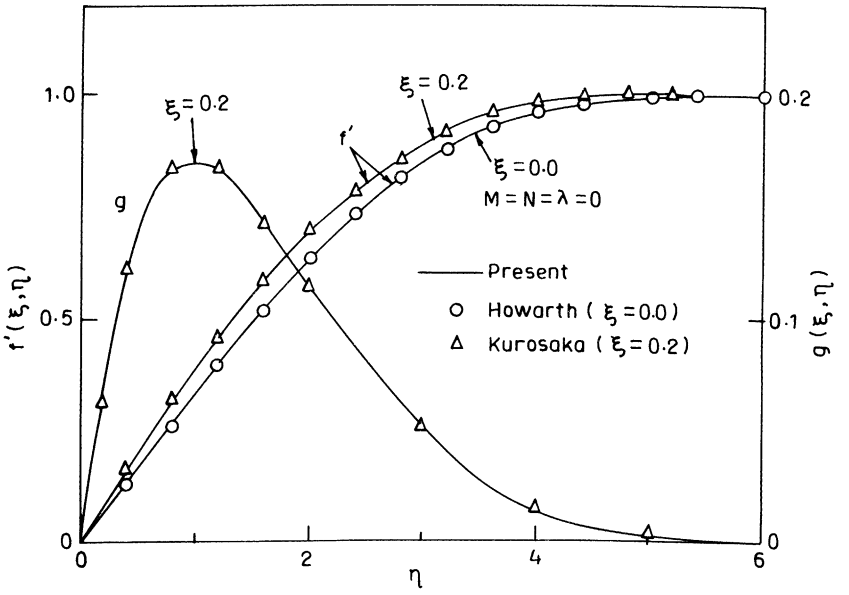

Fig. 2. Comparison of the velocity profile in the primary flow, $f'(\xi,\eta)$, for $\xi = M = N = \lambda = 0$ with that of Howarth [21] and of the velocity profiles in the primary and secondary flows, $f'(\xi,\eta)$, $g(\xi,\eta)$ for $\sigma = 0.2$, $M = N = \lambda = 0$ with those of Kurosaka [6].

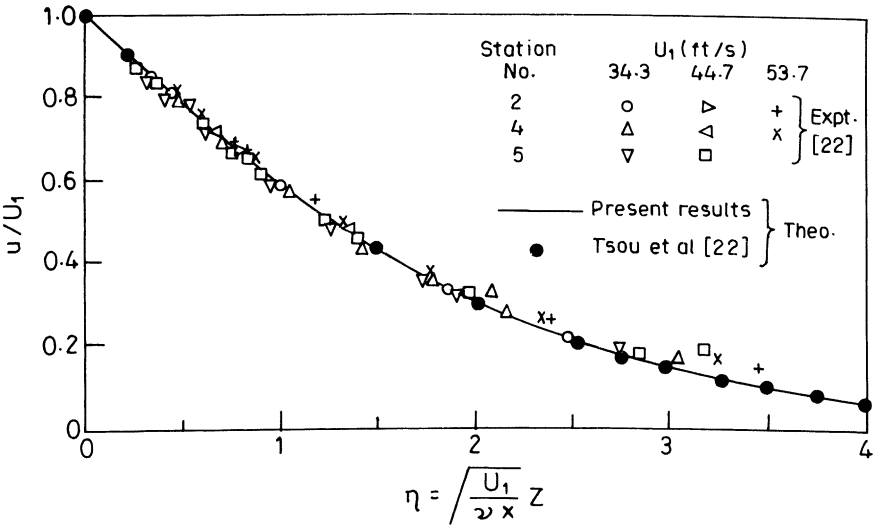

Fig. 3. Comparison of the velocity profile in the primary flow, $u/U_1 = f'(\xi,\eta)$, for $\xi = M = N = 0$, $\lambda = 1$ with that of Tsou et al. [22].

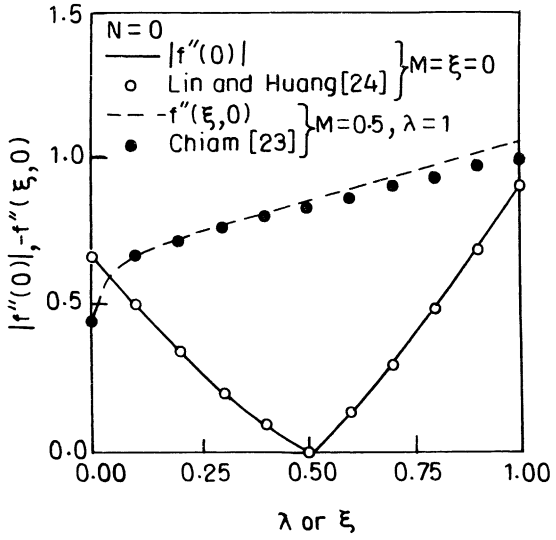

Fig. 4. Comparison of the local skin friction for the primary flow, $-f''(\xi,0)$, for $\lambda = 1$, $N = 0$, $0 \leqslant \xi \leqslant 1$ with that of Chiam [23] and the comparison of $(|f''(0)|$ for $\xi = M = N = 0$, $0 \leqslant \lambda \leqslant 1$ with that of Lin and Huang [24].

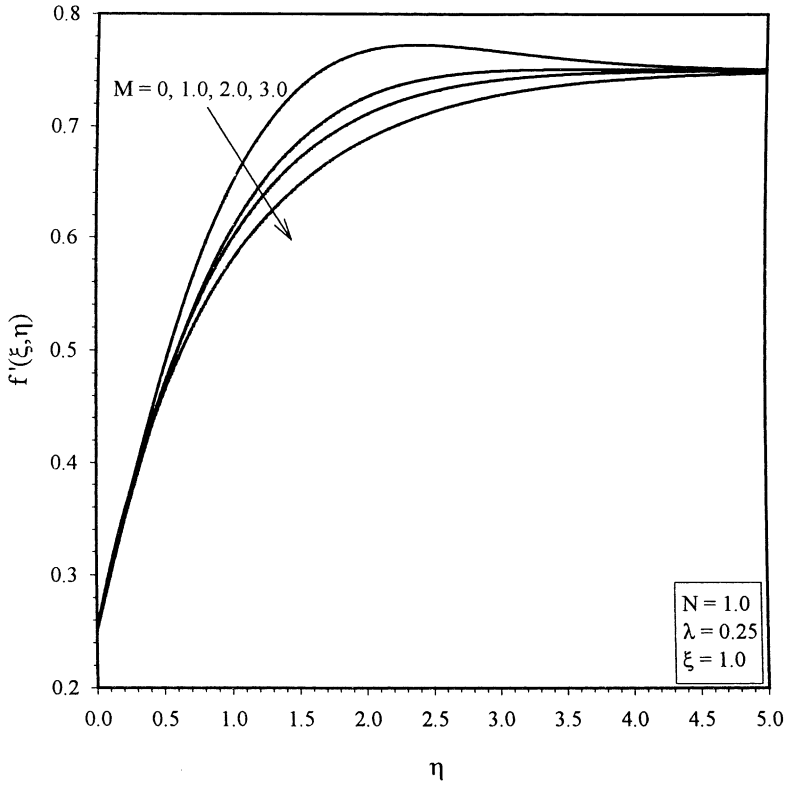

Fig. 5. Effect of the magnetic parameter M on the velocity profiles in the primary flow, $f'(\xi,\eta)$.

Continuity equation:

$$\nabla \cdot \mathbf{V} = 0. \tag{1}$$

Momentum equation:

$$(\mathbf{V} \cdot \nabla)\mathbf{V} + 2\boldsymbol{\Omega} \times \mathbf{V} = -\rho \nabla p + \nu \nabla^2 \mathbf{V} + \rho^{-1}(\mathbf{J} \times \mathbf{B}). \tag{2}$$

Generalized Ohm's law:

$$\mathbf{J} = \sigma(\mathbf{E} + \mathbf{V} \times \mathbf{B}) - (\sigma/en_e)(\mathbf{J} \times \mathbf{B} - \nabla p_e). \tag{3}$$

Maxwell's equations:

$$\nabla \times \mathbf{H} = J, \quad \nabla \times \mathbf{E} = 0, \quad \nabla \cdot \mathbf{B} = 0. \tag{4}$$

Here $\mathbf{V}$ is the velocity vector, $\mathbf{B}$ is the magnetic induction vector, $\mathbf{E}$ is the electric field vector, $\mathbf{H}$ is the magnetic field strength vector, $\mathbf{J}$ is the current density vector, $\boldsymbol{\Omega} = (0, 0, \Omega_0)$ is the angular velocity vector, p is the fluid pressure, p_e electron pressure, ρ is the fluid density, ν is the kinematic

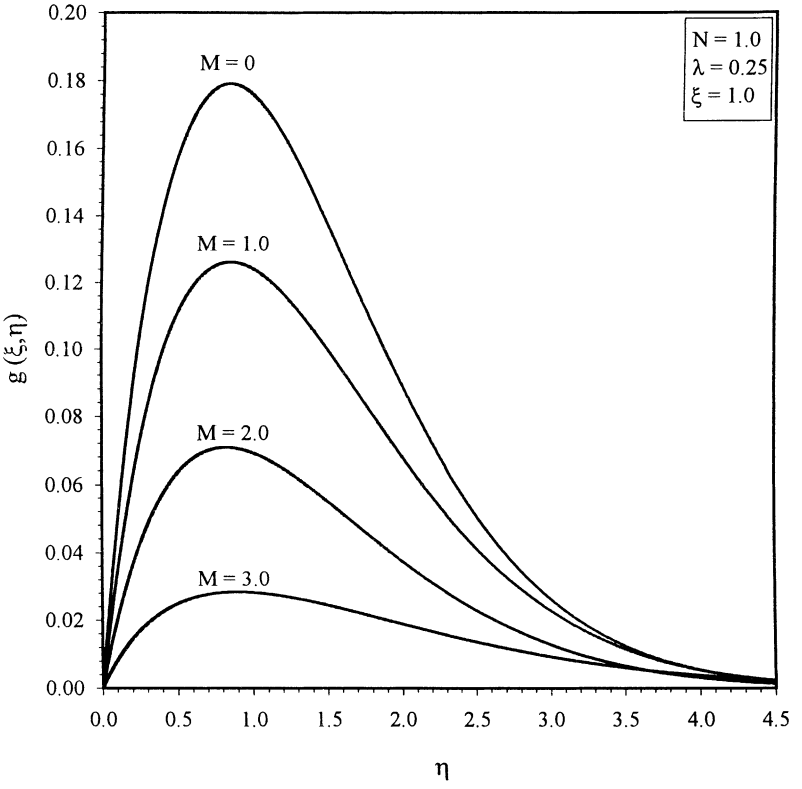

Fig. 6. Effect of the magnetic parameter M on the velocity profiles in the secondary flow, $g(\xi, \eta)$.

viscosity of the fluid, $\sigma(\sigma = (e^2 n_e t_e)/m_e)$ is the electrical conductivity, t_e is the electron collision time, e is the electron charge, n_e is the electron number density, and m_e is the mass of the electron. We assume that the magnetic Reynolds number $Re_m = \mu_0 \overline{V} L \ll 1$, where μ_0 is the magnetic permeability, and $\overline{V}$ and L are characteristic velocity and length, respectively. Under these conditions, it is possible to neglect the induced magnetic field in comparison to the applied magnetic field $\mathbf{B} = (0, 0, B_0)$. Since no applied or polarization voltage is imposed on the flow field, the electric field vector $\mathbf{E} = \mathbf{0}$. If we assume that the magnetic field strength is large, the generalized Ohm's law given by Eq. (3) in the absence of the electric field can be expressed as

$$\mathbf{J} + (\omega_e t_e / B_0)(\mathbf{J} \times \mathbf{B}) = \sigma[\mathbf{V} \times \mathbf{B} + (\nabla p_e / e n_e)], \tag{5}$$

where $\omega_e (= eB_0/m_e)$ is the electron frequency. For weakly ionized gases, the electron pressure gradient and the ion-slip effects (due to imperfect coupling between ions and neutrons) can be neglected. Hence Eq. (5) reduces to

$$\begin{aligned} J_x &= \sigma B_0 (1 + N^2)^{-1} (Nu + v), \\ J_y &= \sigma B_0 (1 + N^2)^{-1} (Nv - u), \end{aligned} \tag{6}$$

where $N (= \omega_e t_e)$ is the Hall parameter.

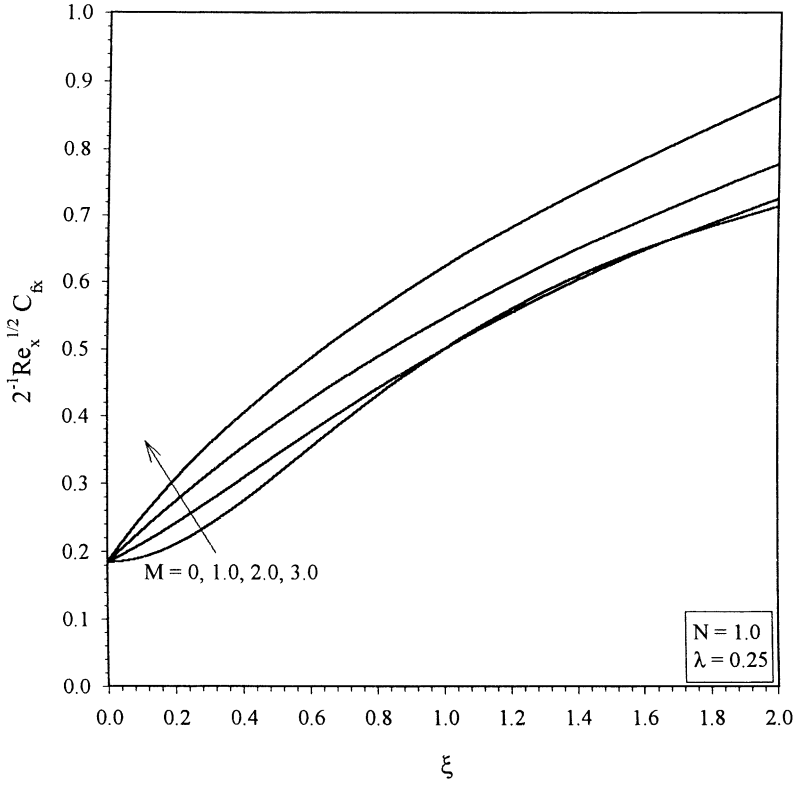

Fig. 7. Effect of the magnetic parameter M on the local skin friction coefficient for the primary flow, $2^{-1} Re_x^{1/2} C_{fx}$.

If we assume that the surface extends to infinity in the y-direction, then the velocity components u, v and w depend on x and z only. Under the above conditions, the boundary layer equations governing the unsteady flow in a rotating frame of reference can be re-written as

Continuity equation:

$$u_x + w_z = 0. \tag{7}$$

Momentum equation:

$$uu_x + wu_z - 2\Omega_0 v = -\rho^{-1}p_x + \nu u_{zz} + (\sigma B_0^2/\rho)(1+N^2)^{-1}(Nv - u), \tag{8}$$

$$uv_x + wv_z + 2\Omega_0 u = -\rho^{-1}p_y + \nu v_{zz} - (\sigma B_0^2/\rho)(1+N^2)^{-1}(Nu + v). \tag{9}$$

Far away from the surface, the pressure gradients in the x and y directions, $-\rho^{-1}\,p_x$ and $-\rho^{-1}\,p_y$, must balance the Lorentz and Coriolis forces and are given by the relations:

$$\begin{aligned} -\rho^{-1}p_x &= (\sigma B_0^2/\rho)(1+N^2)^{-1}U_2, \\ -\rho^{-1}p_y &= 2\Omega_0 U_2 + (\sigma B_0^2/\rho)(1+N^2)^{-1}NU_2. \end{aligned} \tag{10}$$

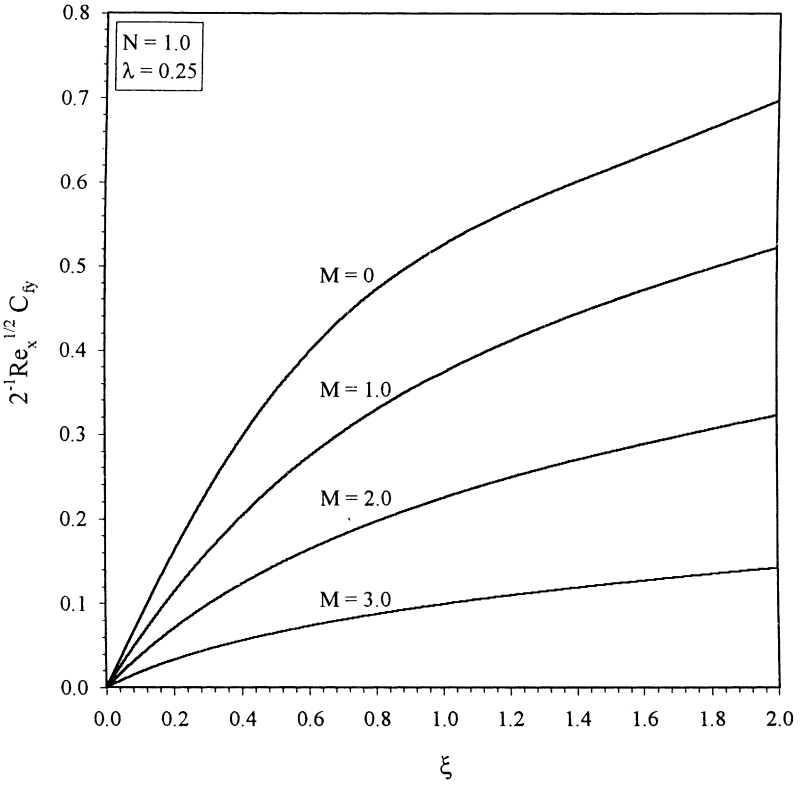

Fig. 8. Effect of the magnetic parameter M on the local skin friction coefficient for the secondary flow, $2^{-1}Re_x^{1/2}C_{fy}$.

The boundary conditions are the no-slip conditions at the surface and the free stream conditions outside the boundary layer. Hence the boundary conditions are given by

$$\begin{aligned} &u(x,0) = U_1, \quad v(x,0) = 0, \quad w(x,0) = 0, \\ &u(x,\infty) = U_2, \quad v(x,\infty) = 0, \\ &u(0,z) = U_2, \quad v(0,z) = 0, \ \ z > 0, \end{aligned} \tag{11}$$

where U_1 and U_2 are the surface and free stream velocities, respectively and the subscripts x and z denote partial derivative with respect to x and z, respectively.

In order to reduce Eqs. (7)–(9) to a convenient form, we introduce dimensionless independent variables (ξ, η) and dimensionless stream function $f(\xi, \eta)$ and dimensionless velocity components $f'(\xi, \eta)$ and $g(\xi, \eta)$ along the x and y directions, respectively and these are expressed as

$$\begin{aligned} &\eta = (U/vx)^{1/2} z, \quad \xi = \Omega_0 x/U, \quad U = U_1 + U_2, \quad u = \partial\psi/\partial z, \quad w = -\partial\psi/\partial x, \\ &\psi(x,z) = (Uvx)^{1/2} f(\xi,\eta), \quad u = Uf'(\xi,\eta), \quad v = Ug(\xi,\eta), \\ &w = -(\Omega_0 v\xi)^{1/2}[(\partial f/\partial\xi) + (2\xi)^{-1}(f - (\Omega_0/U)\eta f')], \quad \lambda = U_1/U, \\ &M = Ha^2/Re_L, \quad Ha^2 = \sigma B_0^2 L^2/\mu, \quad Re_L = UL/v, \end{aligned} \tag{12}$$

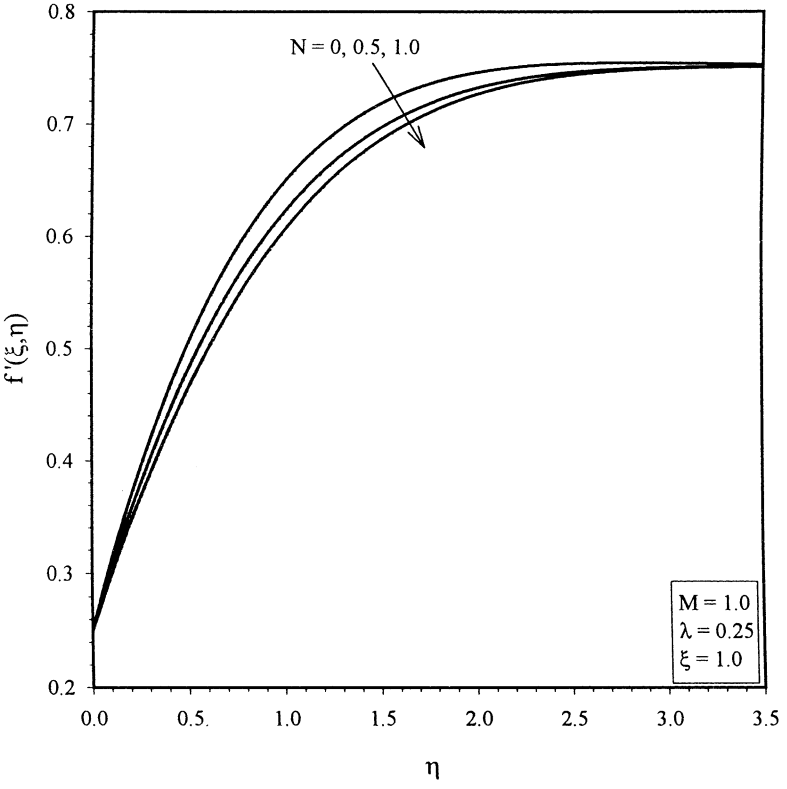

Fig. 9. Effect of the Hall parameter N on the velocity profiles in the primary flow, $f'(\xi, \eta)$.

where prime denotes the derivative with respect to η.

We apply the above transformations to Eqs. (7)–(9) and we find that Eq. (1) is identically satisfied and Eqs. (8) and (9) reduced to

$$f''' + 2^{-1}ff'' + 2\xi g - M(1+N^2)^{-1}\xi(f' - 1 + \lambda - Ng) = \xi(f'\partial f'/\partial\xi - f''\partial f/\partial\xi), \tag{13}$$

$$g'' + 2^{-1}fg' + 2\xi(1 - \lambda - f') - M(1+N^2)^{-1}\xi[g + N(f' - 1 + \lambda)] = \xi(f'\partial g/\partial\xi - g'\partial f/\partial\xi). \tag{14}$$

The boundary conditions (11) can be re-written as

$$f(\xi,0) = 0, \quad f'(\xi,0) = \lambda, \quad g(\xi,0) = 0, \quad f'(\xi,\infty) = 1 - \lambda, \quad g(\xi,\infty) = 0. \tag{15}$$

Here M is the magnetic parameter, Ha^2 is the Hartmann number, Re_L is the Reynolds number, μ is the coefficient of dynamic viscosity, L is the characteristic length, U is the composite velocity, λ is the ratio of the surface velocity to the composite velocity, ξ represents the Coriolis force and it also denotes the distance measured from the leading edge of the surface, and a prime denotes a derivative with respect to η.

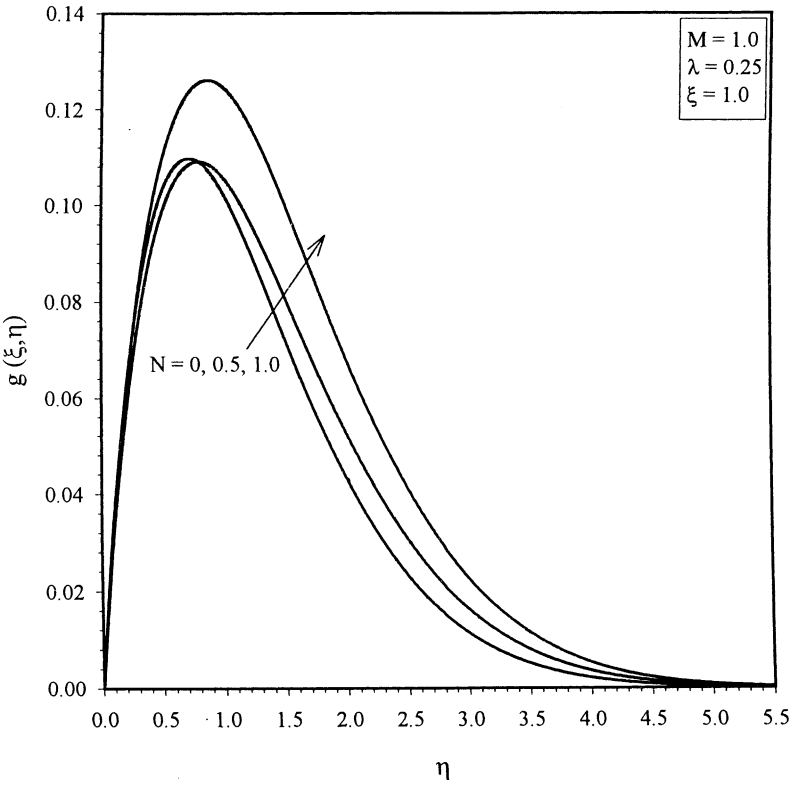

Fig. 10. Effect of the Hall parameter N on the velocity profiles for the secondary flow, $g(\xi,\eta)$.

It may be noted that for $\lambda = 0.5$ (i.e., when surface velocity and free stream velocity are equal), Eqs. (13) and (14) under the boundary conditions (15) admit closed form solutions which are given by

$$f(\xi,\eta) = \eta/2, \quad g(\xi,\eta) = 0. \tag{16}$$

It may be remarked that Eqs. (13)–(15) for $M = N = \lambda = 0$ (without the magnetic field and Hall currents on a stationary surface) reduce to those of Kurosaka [6]. For $\xi = M = N = 0$, $\lambda = 0$ and 1, Eq. (13) represents the flow over a stationary surface (Blasius flow) and over a moving surface in an ambient fluid which are giver in [21,22], respectively. For ξ (without the Coriolis force), $g(\xi,\eta) = 0$ and Eq. (14) is not required. Further, Eq. (13) for $\lambda = 1$, $N = 0$ reduces to that of Chiam [23] who considered the MHD flow over a moving surface if we replace ξ by x and omit the term $2\xi g$ (which arises due to the rotation of the fluid). Also Eq. (13) for $\xi = M = N = 0$ reduces to that of Lin and Huang [24].

The local skin friction coefficients in the x and y directions can be expressed as

$$\begin{aligned} C_{fx} &= 2\mu(\partial u/\partial z)_{z=0}/\rho U^2 = 2(Re_x)^{-1/2} f''(\xi,0), \\ C_{fy} &= 2\mu(\partial v/\partial z)_{z=0}/\rho U^2 = 2(Re_x)^{-1/2} g''(\xi,0), \end{aligned} \tag{17}$$

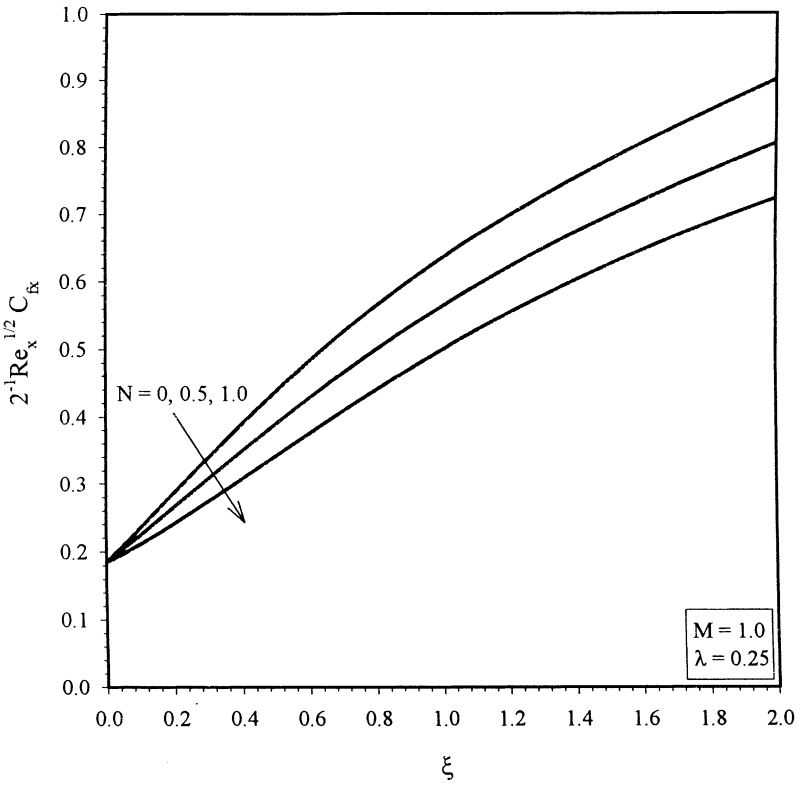

Fig. 11. Effect of the Hall parameter N on the local skin friction coefficient for the primary flow, $2^{-1}Re_x^{1/2}C_{fx}$.

where C_{fx} and C_{fy} are the local skin friction coefficients in the x and y directions, respectively (for the primary and secondary flows) and $Re_x = Ux/v$ is the local Reynolds number.

3. Method for solution

The nonlinear coupled parabolic partial differential equations (13) and (14) under the boundary conditions (15) have been solved by using an implicit, iterative, tri-diagonal finite-difference scheme similar to that of Blottner [20]. All the first-order derivatives with respect to ξ are replaced by two-point backward difference formulae

$$\partial R/\partial\xi = (R_{i,j} - R_{i-1,j})\Delta\xi, \tag{18}$$

where R represents dependent variable f or g and i and j are the node locations along the ξ and η directions, respectively. First the third-order partial differential equation (13) is converted to a second-order equation by substituting $f' = F$, then the second-order derivatives with respect to η for F and g are discretized using three-point central-difference formulae while the first-order derivatives are discretized by employing the trapezoidal rule. At each line of constant ξ, a system of

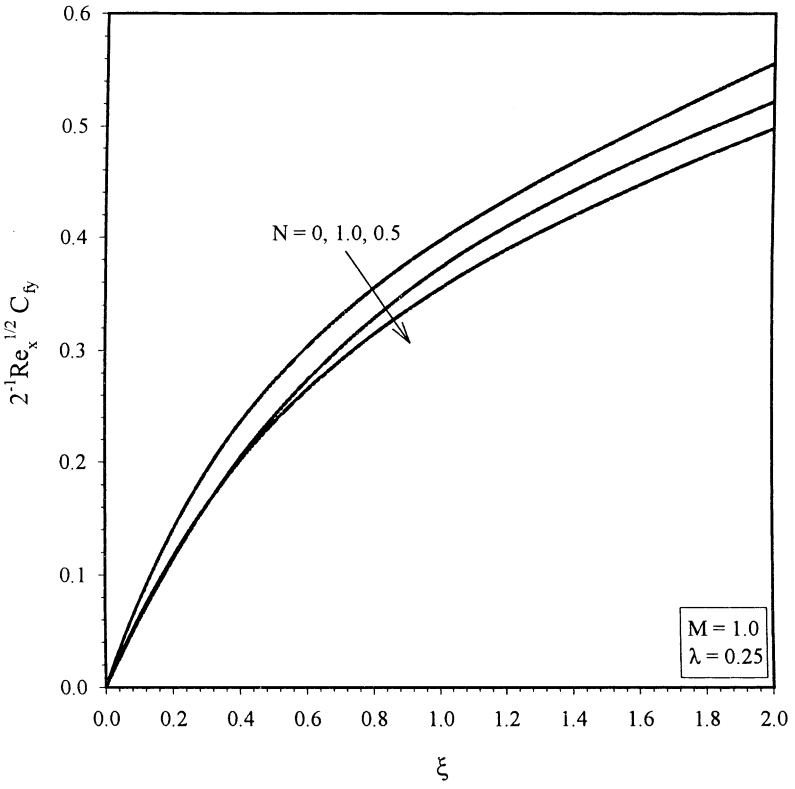

Fig. 12. Effect of the Hall parameter N on the local skin friction coefficient for the secondary flow, $2^{-1}Re_x^{1/2}C_{fy}$.

algebraic equation is obtained. The nonlinear terms are evaluated at the previous iteration and the equations are solved iteratively by using the Thomas algorithm (see [20]). The same procedure is followed for the next ξ value and the equations are solved line by line until the desired ξ value is reached. A convergence criterion based on the relative difference between the current and the previous iterations is used. When this difference reaches 10^{-5}, the solution is assumed to have converged and the iterative process is terminated.

4. Results and discussion

Eqs. (13) and (14) under the boundary conditions (15) have been solved by using an implicit finite-difference scheme as described earlier. In order to validate our results, we have compared the velocity profile $f'(\eta)$ for $\xi = \lambda = M = N = 0$ with that of Howarth as given by Schlichting [21]. We have also compared the velocity profiles in the primary and secondary flows ($f'(\xi,\eta)$, $g(\xi,\eta)$) for $\xi = 0.2$, $M = N = \lambda = 0$ with those of Kurosaka [6]. In both the cases, the results are found to be in good agreement. The comparison is shown in Fig. 2. For $\lambda = 1$, $\xi = M = N = 0$, we have compared the velocity profile $u/U_1 = f'(\eta)$ with the theoretical and experimental results of Tsou et al. [22]. This comparison is given in Fig. 3. It is in very good agreement with the theoretical

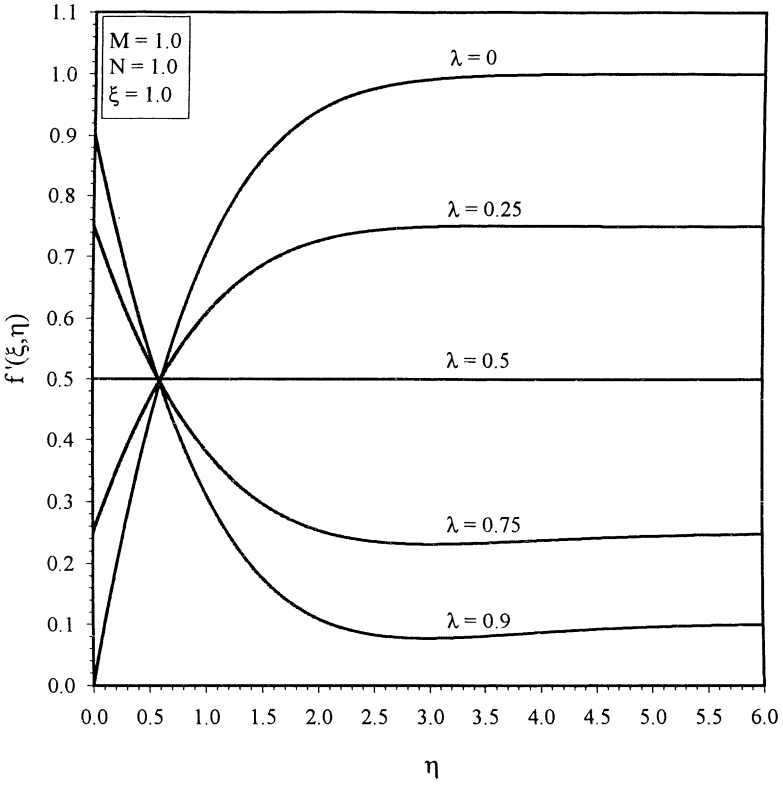

Fig. 13. Effect of the wall velocity λ on the velocity profiles for the primary flow, $f'(\xi,\eta)$.

values and it also agrees well with the experimental values near the wall. We have also compared the local skin friction $(-f''(\xi,0))$ for $\lambda = 1, M = 0.5, N = 0, 0 \leqslant \xi \leqslant 1$ with that of Chiam [23] who solved the governing equations using an approximate method (local non-similarity method). Further, we have compared the local skin friction $(|f''(0)|)$ results for $\xi = M = N = 0, 0 \leqslant \lambda \leqslant 1$ with those of Lin and Huang [24]. For both the cases, the comparison is presented in Fig. 4. The results are found to be in excellent agreement with those of Lin and Huang [24], but for large ξ these results slightly differ from those of Chiam [23]. This difference is attributed to the approximate method used by Chiam.

The effect of the magnetic parameter M on the velocity profiles for the primary and secondary flows $(f'(\xi,\eta), g(\xi,\eta))$ for $\xi = N = 1, \lambda = 0.25$ is shown in Figs. 5 and 6. The velocity profile in the primary flow $(f'(\xi,\eta))$ for $M = 0, \xi = 1$ exceeds its value at the edge of the boundary layer (i.e., there is a velocity overshoot). This velocity overshoot is due to the Coriolis force which supports the motion. Since the magnetic field has a stabilizing effect, the velocity overshoot decreases with increasing M and if $M \geqslant M_0$, the overshoot in the velocity vanishes. The maximum or peak velocity in the secondary flow $(g(\xi,\eta))$ decreases with increasing M. As mentioned earlier, the reason for this trend is due to the stabilizing effect of the magnetic field.

The effect of the magnetic parameter M on local skin friction coefficients for the primary and secondary flows $(2^{-1}Re_x^{1/2}C_{fx},\ 2^{-1}Re_x^{1/2}C_{fy})$ for $N = 1,\ \lambda = 0.25,\ 0 \leqslant \xi \leqslant 2$ has been presented in

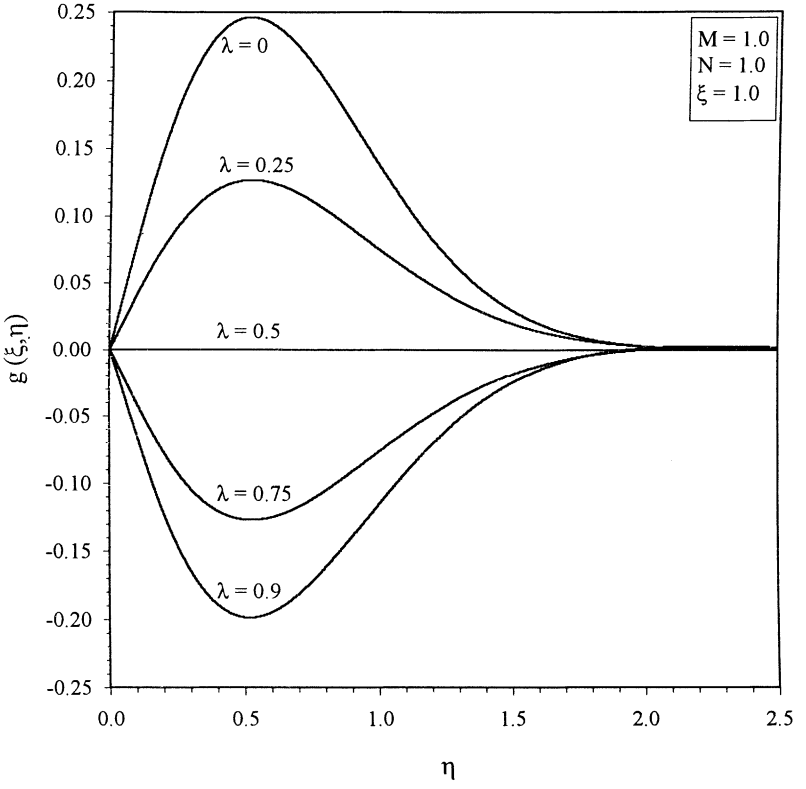

Fig. 14. Effect of the wall velocity λ on the velocity profiles for the secondary flow, $g(\xi,\eta)$.

Figs. 7 and 8, respectively. For a fixed ξ, the skin friction coefficient for the primary flow increases with the magnetic parameter M, but the skin friction coefficient for the secondary flow decreases. This is due to the stabilizing effect of the magnetic field which increases the velocity in the primary flow, but reduces the velocity in the secondary flow. For $N = 1$, $\xi = 2$, the skin friction coefficient for the primary flow increases by about 24% as M increases from zero to four, but the skin friction coefficient for the secondary flow decreases by about 80%. Similarly, for a fixed M the skin friction coefficients for the primary and secondary flows increase with the Coriolis force (ξ). The reason for this behaviour is that the Coriolis force assists the fluid motion which results in an increase in the velocity gradients in the primary and secondary flows and hence in the skin friction coefficients for the primary and secondary flows. For $M = 3$, $N = 1$, $\lambda = 0.25$, the skin friction coefficients for the primary and secondary flows increase by about 93% and 100%, respectively, as ξ increases from zero to two.

The effect of the Hall parameter N on the velocity profiles for the primary and secondary flows $(f'(\xi,\eta), f(\xi,\eta))$ for $M = \xi = 1$, $\lambda = 0.25$ is displayed in Figs. 9 and 10, respectively. The velocity profile $f'(\xi,\eta)$ becomes less steep as N increases. The velocity for the secondary flows $g(\xi,\eta)$ attains its maximum value near the wall and this value increases with N.

Figs. 11 and 12, respectively, present the effect of the Hall parameter N on the skin friction coefficients for the primary and secondary flows $(2^{-1}Re_x^{1/2}C_{fx}, 2^{-1}Re_x^{1/2}C_{fy})$ for $M = 1$, $\lambda = 0.25$,

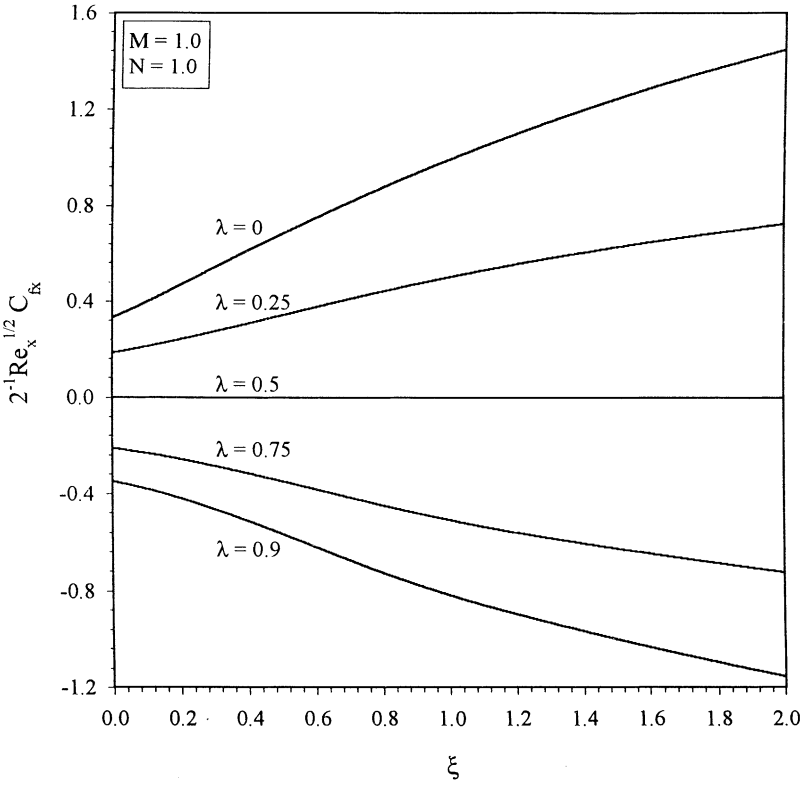

Fig. 15. Effect of the wall velocity λ on the local skin friction coefficient for the primary flow, $2^{-1}Re_x^{1/2}C_{fx}$.

$0 \leqslant \xi \leqslant 2$. The skin friction coefficients reduce with increasing N. This trend is attributed to the destabilizing effect of the Hall current. For $M = 1$, $\lambda = 0.25$, $\xi = 2$, the skin friction coefficients for the primary and secondary flows decrease by about 22% and 6%, respectively, as N increases from zero to one.

Figs. 13 and 14 show the effect of the ratio of the wall velocity to the composite velocity represented by the parameter λ on the velocity profiles in the primary and secondary flows $(f'(\xi,\eta), g(\xi,\eta))$ for $M = N = \xi = 1$. It is observed that λ exerts a strong influence on the velocity profiles. It can be seen that for any two values of λ, the velocity profiles in the primary flow, $f'(\xi,\eta)$, cross each other near the wall $(\eta = 0.5)$. For $\lambda < 0.5$, $f'(\xi,\eta)$ increases with η, but for $\lambda > 0.5$ it decreases. Also the velocity profiles in the secondary flow $g(\xi,\eta) > 0$ for $\lambda < 0.5$, but it is <0 for $\lambda > 0.5$. For $\lambda = 0.5$, $f(\xi,\eta) = \eta/2$, $g(\xi,\eta) = 0$ as mentioned earlier (see Eq. (16)).

Figs. 15 and 16 display the effect of the parameter λ on the local skin friction coefficients for the primary and secondary flows $(2^{-1}Re_x^{1/2}C_{fx}, 2^{-1}Re_x^{1/2}C_{fy})$ for $M = N = 1$, $0\xi \leqslant 2$. These coefficients are positive for $\lambda < 0.5$ and negative for $\lambda > 0.5$. For $\lambda > 0.5$ the velocities $f'(\xi,\eta)$ and $g(\xi,\eta)$ increase with η, but for $\sigma > 0.5$ these decrease (see Figs. 13 and 14). For $\lambda = 0.5$, the skin friction coefficients vanish for all ξ, M and N, but it does not imply separation, because we are considering the moving wall problem. For $\lambda > 0.5$, the fluid is being dragged by the plate, but for $\lambda < 0.5$ the plate is being dragged by the fluid.

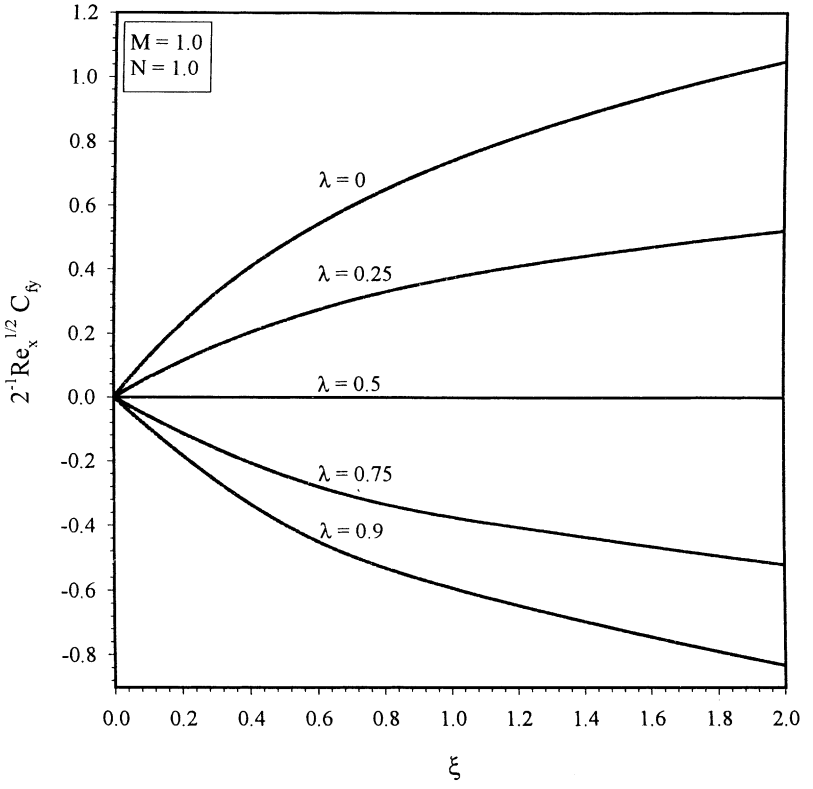

Fig. 16. Effect of the wall velocity λ on the local skin friction coefficient for the secondary flow, $2^{-1}Re_x^{1/2}C_{fy}$.

5. Conclusions

The Coriolis force causes overshoot in the velocity profiles of the primary flow and the velocity overshoot is reduced/removed by the application of the magnetic field. The local skin friction coefficient for the primary flow increases with the magnetic field, but the local skin friction coefficient for the secondary flow decreases, whereas both these coefficients decrease with increasing Hall currents. Also the skin friction coefficient in the primary and secondary flows increase with the Coriolis force. The wall velocity strongly affects the primary and secondary flow fields. When the wall velocity and the free stream velocity are equal, the skin friction coefficients for the primary and secondary flow vanish, but no fluid separation occurs.

References

[1] R. Hide, P.H. Roberts, The origin of the mean geomagnetic field, in: Physics and Chemistry of the Earth, vol. 4, Pergamon Press, New York, 1961, pp. 27–98.
[2] R.H. Dieke, Internal rotation of the sun, in: L. Goldberg (Ed.), Annual Reviews of Astronomy and Astrophysics, vol. 8, Annual Reviews Inc, 1970, pp. 297–328.
[3] R.S. Nanda, H.K. Mohanty, Hydromagnetic rotating channel flows, Appl. Sci. Res. A 24 (1970) 65–75.
[4] A.S. Gupta, Ekman layer on a porous plate, Phys. Fluids 15 (1972) 930–931.
[5] L. Debnath, On unsteady MHD boundary layers in a rotating flow, Recent Research in Unsteady Boundary Layers, Les Presses De L'Université Laval, Quebec, 1972.
[6] M. Kurosaka, The oscillatory boundary layer growth over the top and bottom plates of a rotating channel, J. Fluid Eng. 95 (1973) 68–71.
[7] I. Pop, V.M. Soundelgekar, On unsteady boundary layers in rotating flow, J. Inst. Math. Appl. 15 (1975) 343–349.
[8] L. Debnath, Exact solutions of the unsteady hydrodynamic and hydromagnetic boundary layer equations in a rotating fluid system, ZAMM 55 (1975) 431–438.
[9] G. Sarojamma, D.V. Krishna, Transient hydromagnetic convective flow in rotating channel with porous boundaries, Acta Mech. 43 (1981) 49–54.
[10] E.M. Smirnov, A.V. Shatrov, Development of the boundary layer on a plate in a rotating system, Fluid Dyn. 17 (1982) 452–454.
[11] M.A. Page, The low Rossby number flow of a rotating fluid past a flat plate, J. Eng. Math. 17 (1983) 191–202.
[12] C.Y. Wang, Stretching a surface in a rotating fluid, ZAMP 39 (1988) 177–185.
[13] H.S. Takhar, G. Nath, Unsteady flow over a stretching surface with a magnetic field in a rotating fluid, ZAMP 49 (1998) 989–1001.
[14] H. Sato, The Hall effect in the viscous flow of ionized gas between parallel plates under a transverse magnetic field, J. Phys. Soc. Jpn. 16 (1961) 1427–1433.
[15] M. Katagiri, The effect of Hall current on the MHD boundary layer flow past a semi-infinite plate, J. Phys. Soc. Jpn. 27 (1969) 1051–1059.
[16] B.N. Rao, M.L. Mittal, H.R. Nataraja, Hall effect in a boundary layer flow, Acta Mech. 49 (1983) 148–151.
[17] M.A. Hossain, Effect of Hall current in unsteady hydromagnetic free convection flow near an infinite vertical porous plate, J. Phys. Soc. Jpn. 55 (1986) 2183–2190.
[18] M.A. Hossain, R. Rashid, Hall effects in hydromagnetic free convection flow along a porous flat plate with mass transfer, J. Phys. Soc. Jpn. 56 (1987) 97–104.
[19] M. Acharya, G.C. Dash, L.P. Singh, Effect of chemical and thermal diffusion with Hall current in unsteady hydromagnetic flow near an infinite vertical porous plate, J. Phys. D 28 (1995) 2455–2464.
[20] F.G. Blottner, Finite-difference method of solution of the boundary layer equations, AIAA J. 8 (1970) 193–205.
[21] H. Schlichting, Boundary-Layer Theory, seventh ed., McGraw-Hill, New York, 1979.
[22] F.K. Tsou, E.M. Sprrow, R.J. Goldstein, Flow and heat transfer in the boundary layer in a continuously moving surface, Int. J. Heat Mass Transfer 10 (1967) 219–235.

[23] T.C. Chiam, Magnetohydrodynamic boundary layer flow due to a continuously moving flate plate, Comp. Math. Appl. 26 (1993) 1–7.
[24] H.T. Lin, S.F. Huang, Flow and heat transfer of plane surfaces moving in parallel and reversely in the free stream, Int. J. Heat Mass Transfer 37 (1994) 333–336.
[25] A.C. Eringen, G.A. Maugin, Electrodynamics of Continua, vol. 2, Springer, Berlin, 1990.